Correlation Between Catalytic Activity and Metal Cation Coordination: NO Decomposition Over Cu/Zeolites

2 AUTHORS:

Angeles Pulido
University of Southampton
24 PUBLICATIONS **450** CITATIONS

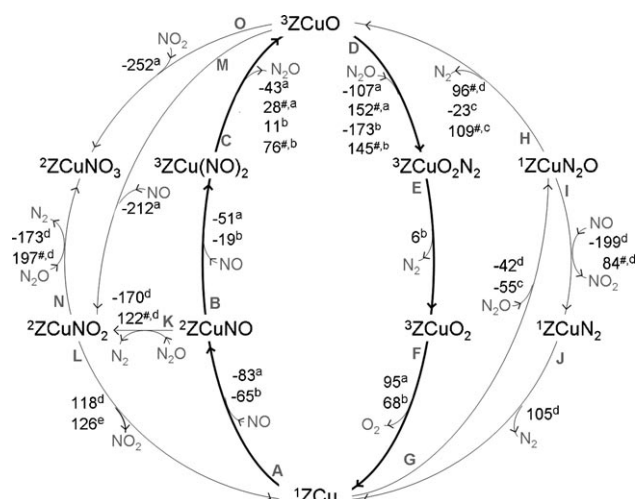Petr Nachtigall
Charles University in Prague
141 PUBLICATIONS **3,562** CITATIONS

Correlation Between Catalytic Activity and Metal Cation Coordination: NO Decomposition Over Cu/Zeolites

Angeles Pulido[a] and Petr Nachtigall*[b]

Since Iwamoto's discovery of an unusually high activity of Cu/zeolites in NO decomposition,[1] there has been an ongoing experimental and theoretical quest to understand the details of the mechanism of this process. Despite this tremendous effort, there are still a number of unsettled questions, including the uncertainty about the nature of the reaction intermediates and about the structure of the active site;[2] either the involvement of only a single extra-framework Cu cation[3–8] or the concerted effect of two nearby Cu cations, the Cu pair,[9–14] was proposed. From the vast amount of relevant experimental data available today, it is clear that the activity of the Cu/zeolite catalysts depends on 1) zeolite topology, 2) zeolite composition (Si/Al ratio and Cu loading), and 3) Cu-exchange procedure, including the sample pretreatment.[4,6,8,12,13,15] However, the understanding of the relationship between active site structure (the metal coordination and localization) and catalytic activity is far from complete; it is our goal to increase our knowledge in this respect.

The lack of direct experimental evidence about the transition-state structures and about the details of the reaction mechanism justifies the use of quantum chemistry to provide the missing details. However, a reliable description of the reactions catalyzed by transition metals in a complex environment (such as zeolites) represents a major challenge for contemporary computational chemistry since it requires the use of a model that realistically represents the active site (including its environment) and the use of a method that can consistently describe the electronic structure of the system along the reaction path (see the Methods section). Many reaction steps possibly involved in the direct NO decomposition on Cu/zeolites have been investigated previously by employing various models and methods.[16–20] Several reaction paths proposed in the literature have been compiled (Scheme 1) along with the reaction energies and activation barriers (where available) reported for the elementary reaction steps. Since these energies were obtained at various levels of theory using different types of models for the active site, a direct comparison should be taken with some caution. For example, the reaction energies of −107 and −173 kJ mol^{-1} were reported for reaction step D

[a] Dr. A. Pulido
Institute of Organic Chemistry and Biochemistry
ASCR, v.v.i., Flemingovo nám. 2, 16610 Prague 6 (Czech Republic)

[b] Prof. P. Nachtigall
Department of Physical and Macromolecular Chemistry
Faculty of Science, Charles University in Prague
Hlavova 2030, 12840 Prague 2 (Czech Republic)
Fax: (+ 420) 220-410-320
E-mail: petr.nachtigall@molecular.cz

Scheme 1. A schematic representation of the possible processes taking place during NO removal in zeolites. The reaction energies and activation barriers (denoted by #) are taken from the literature: a) Ref. [16], b) Ref. [17], c) Ref. [18], d) Ref. [19], and e) Ref. [20]. Superscript numbers refer to the spin multiplicity of the adsorption complex.

based on the BP86 functional (using a 1-T cluster model) and based on the B3LYP functional (using a 3-T cluster model), respectively.[16,17]

A majority of the proposed reaction mechanisms start with the interaction of two NO molecules with Cu/zeolite (ZCu) producing ZCuO and N$_2$O (A→B→C). Different routes were proposed for the subsequent conversion of N$_2$O: 1) it can interact with another NO molecule to produce N$_2$ and NO$_2$. One of the G→I→J, A→K→L, or M→L routes can be followed; the rate-determining steps of these reaction routes are characterized with activation barriers of 105,[18] 122,[19] and 126 kJ mol^{-1}[20], respectively. 2) N$_2$O can be reattached to ZCu to release N$_2$ while forming another ZCuO species (process G→H).[18,19] Note however, that all these reaction paths lead to the production of NO$_2$ and/or ZCuO species. To close the catalytic cycle, the ZCuO needs to be reduced back to ZCu and the NO$_2$ must further react. However, NO$_2$ can readily interact with ZCuO forming ZCuNO$_3$ (process O; $\Delta E = -252$ kJ mol^{-1}).[16] It is not clear how to proceed from a stable ZCuNO$_3$ complex towards the products.

Another route was proposed following the A→B→C path:[16,17] a simple reaction mechanism based on the re-adsorption of N$_2$O on ZCuO (through the O-end) that leads to the formation of N$_2$, O$_2$, and ZCu (D→E→F). An activation barrier for the rate-determining step on this path (the formation of ZCuO$_2$N$_2$) of 152 and 145 kJ mol^{-1} has been reported based on BP86/(1-T cluster)[16] and B3LYP/(3-T cluster)[17] calculations, respectively. Whereas the activation barrier of the D→E→F

path is larger than that for the alternative reaction paths described above, the reaction path A→B→C→D→E→F still appears to be the most attractive one, as it does not require a subsequent reduction of the ZCuO species.

Based on the reasons outlined above, we have focused on the detailed investigation of the A→B→C→D→E→F catalytic cycle using, for the first time, a periodic DFT model that fully accounts for the effect of the zeolite lattice on the stability of the reaction intermediates. The goals of this study include: 1) the localization and characterization of the reaction intermediates and the transition-state structures in the triplet electronic state and 2) the investigation of the effect of the active copper site localization and coordination on the reaction profile. Whereas the majority of the experimental work on direct NO decomposition in Cu/zeolites has been carried out on Cu/ZSM-5 zeolite, for computational reasons we have investigated this reaction mainly in Cu/FER (which also shows catalytic activity[15] but has a unit cell of a size more suitable for a computational investigation). Only a few calculations have been performed for the Cu/ZSM-5 zeolite.

The structure and stability of various dinitrosyl complexes have been investigated recently[21] for four stable Cu^I sites in Cu/FER (Figure 1). The reaction path is first discussed for Cu^I at the M7/T3 site that has been shown to form the most stable dinitrosyl complexes.[21] The relative energies calculated at the Perdew–Burke–Ernzerhof (PBE), B3LYP, and coupled clusters [CCSD(T)] levels are reported (Figure 2a; see the Supporting Information). Unless stated otherwise, the $\Delta E_{CCSD(T)}$ values are reported in the following text. The catalytic cycle starts with the formation of the O-down mononitrosyl complex **1**. The interaction with the second NO molecule leads to the cyclic dinitrosyl complex **3**, $Cu(N_2O_2\text{-}\kappa^2O,O')$, that is formed through TS **2**. As is apparent from Figure 2a, the N—N bond is partially

Figure 2. The relative energies of the complexes along the reaction path A→B→C→D→E→F. a) The energies calculated at the PBE, B3LYP, and CCSD(T) levels (depicted in blue, green, and black, respectively) for a reaction taking place on Cu^I at M7/T3 in Cu/FER; the geometries of reaction intermediates are shown in Å (the Cu, N, and O atoms are depicted in yellow, blue, and red, respectively). b) The energies calculated at the CCSD(T) level for the reaction taking place on Cu^I at P6/T1, I2/T2, P8/T4, and M7/T3 in Cu/FER, Cu^I at I2/T12 in Cu/MFI; and on a 1-T cluster model.

formed in complex **3** and the N—O bond is weaker in complex **3** when compared to the gas phase NO or to the mononitrosyl complex **1**. The formation of ZCuO and the N_2O molecule **5** is initiated by breaking one of the N—O bonds (TS **4**). While the reaction **3**→**5** is only slightly endothermic ($\Delta E_{CCSD(T)} = 20$ kJ.mol^{-1}), the TS **4** is 109 kJ mol^{-1} above **3**; however, TS **4** is only 35 kJ mol^{-1} above the reactants. The rate-determining step is a re-attachment of N_2O to ZCuO (via the O-atom of N_2O) that leads to TS **6** (which is 186 kJ mol^{-1} above **5**). TS **6** leads to the release of N_2 and the formation of ZCuO$_2$ **7**. The catalytic cycle is closed by O_2 desorption, which is the elementary step that is 71 kJ mol^{-1} (endothermic). The barrier for the rate determining step **5**→TS **6**→**7** is high. However, an apparent barrier, defined as the difference between the energy of the reactants and the energy of TS **6**, is somewhat smaller (140 kJ mol^{-1}).

The relative stabilities of the stationary points on the reaction path (following the A→B→C→D→E→F route) calculated for various Cu^I sites are shown in Figure 2b. The relative
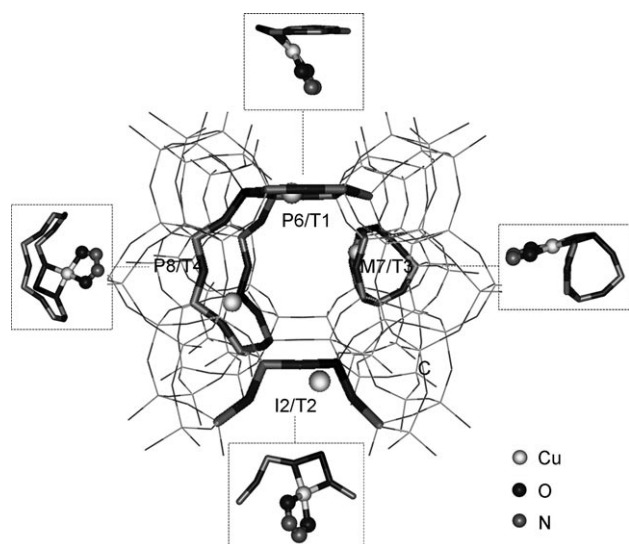

Figure 1. The coordination and localization of Cu^I cations in various sites in Cu/FER is depicted in the central part; the structure of the $(Cu(N_2O_2\text{-}\kappa^2O,O')$ intermediate (complex **3**) on Cu^I sites in Cu/FER is also shown. The Cu, O, and N atoms are depicted as white, dark grey, and grey spheres, respectively; and framework Al, Si, and O atoms are shown in black, grey, and dark grey, respectively.
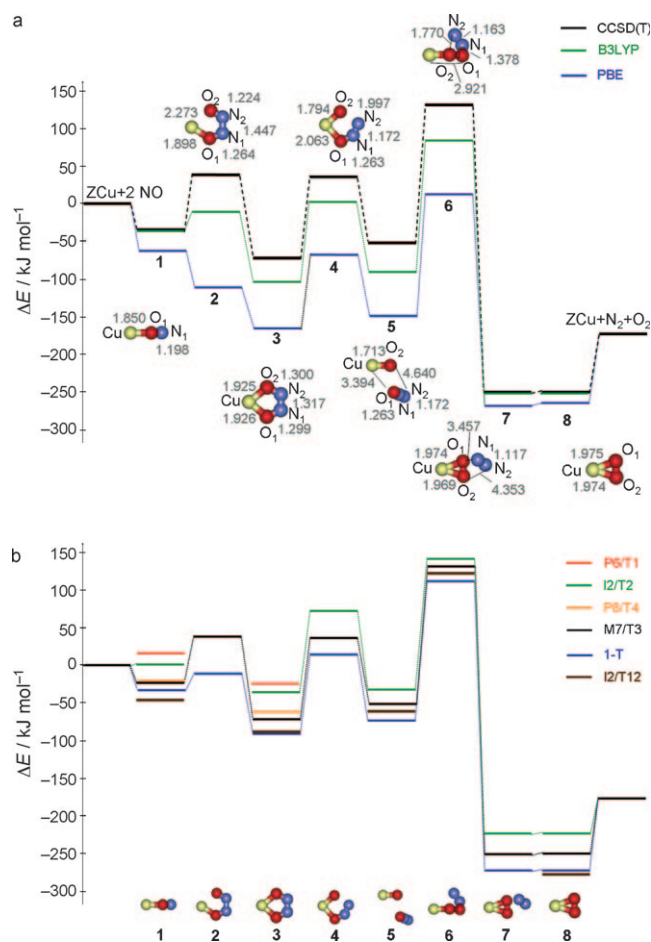
energies of intermediates **1**–**8** are very similar for all of the Cu^I sites investigated. The geometries of the individual reaction intermediates are also rather similar for all of the Cu^I sites. Consequently, the activation barriers for the elementary steps do not depend much on the Cu^I site. However, the energy profiles obtained for individual Cu^I sites are shifted with respect to the energy of the reactants (or products) depending on the coordination of the Cu^I site prior to the interaction with any gas-phase molecule (reaction step A in Scheme 1). Thus, the energy profile of the reaction depends on the Cu^I site in zeolites; the better the coordination of Cu^I with the zeolites framework, the less stable the resulting adsorption complexes.[21] The differences between the Cu^I sites can be related to the framework deformation energies previously calculated for the NO adsorption complexes in Cu/FER:[21] 33, 49, 57, and 66 kJ mol^{-1} for Cu^I in the M7/T3, P8/T4, I2/T2, and P6/T1 sites, respectively (at the PBE level, considering the O-down complex). Apparently, the larger the framework deformation energy, the smaller the stability of the adsorption complexes (Figure 2 b). Thus, the apparent barrier for the process depends on the Cu^I site and is smaller for sites characterized by a smaller deformation energy. In addition, the Cu^I sites having a large deformation energy (P6/T1 in particular) cannot form stable reaction intermediates (complex **1** on P6/T1 has $\Delta E_{CCSD(T)} = 16$ kJ mol^{-1}), making it much less likely that a reaction will take place on them. The correlation between the active-site structure and catalytic activity is of fundamental interest; along with the knowledge of preferred cation sites in various (zeolite) environments, it can explain the differences between the catalytic activities of various catalysts.

It follows that the most active among the Cu/zeolite catalysts are those with Cu^I only loosely coordinated to the zeolite framework. Catalytic activity decreases with improved Cu^I–framework coordination, and Cu^I coordinated inside a flexible (non-bridged) six-membered ring (such as the P6/T1 site) shows lower or no activity. It is known from a previous investigation[22] that, at the intersection of two large (ten-membered ring) channels of ZSM-5, the Cu^I ion is coordinated to only two framework oxygen atoms nonlinearly. Consequently, it forms stable complexes with NO or other molecules;[6,23,24] the framework deformation energy calculated for this site is only 2 kJ mol^{-1}. Therefore, the stability of the reaction intermediates **1**, **3**, **5**, and **8** and TS **6** formed on Cu^I at the intersection I2/T12 site in Cu/ZSM-5 (see Figure 3 in Ref. [22] for details) was investigated at the same level of theory as was used for Cu/FER. Complexes **1**, **3**, **5**, and, **8** have $\Delta E_{CCSD(T)}$ −48, −90, −63, and −280 kJ mol^{-1}, respectively, which means they are 9–27 kJ mol^{-1} more stable than the corresponding complexes formed on the most active Cu^I site (M7/T3) in Cu/FER. Due to computational limitations, we were only able to obtain an estimate for the TS **6** structure in Cu/ZSM-5 (122 kJ mol^{-1}). These calculations nevertheless show that the apparent barrier for the deNO$_x$ process, catalyzed by Cu^I at the intersection site of Cu/ZSM-5, is smaller (by about 10 kJ mol^{-1}) than that of Cu/FER.

The experimental apparent activation barriers for direct NO decomposition taking place on Cu/ZSM-5 are in the range of 90–120 kJ mol^{-1},[25,26] depending on the Si/Al ratio and Cu loading. This is in fair agreement with the calculated barrier of 131 kJ mol^{-1} (ΔH values are reported in the Supporting Information). A comprehensive study of N$_2$O removal catalyzed by several zeolites (including Cu/FER and Cu/ZSM-5) with different Cu/Si/Al ratios was recently reported by Smeets et al.[13] They reported an apparent activation energy of 150 and 138 kJ mol^{-1} for Cu/FER with 0.21 and 0.42 Cu/Al ratio, respectively, and an apparent activation energy of 112–130 for Cu/MFI with various Cu loadings. Assuming that this reaction proceeds via the G→H→D→E→F catalytic cycle (Scheme 1) and considering the stability of the N$_2$O and NO reactants,[27] the apparent energy of activation for N$_2$O removal should be just 11 kJ mol^{-1} larger than for NO removal. The apparent activation energies calculated for the corresponding process for Cu/FER are 151–158 kJ mol^{-1} and about 142 kJ mol^{-1} for Cu/MFI, which are in reasonable agreement with the experimental data.

The periodic DFT model (employed in the present study) is expected to mimic the real system reliably. However, the methods used for the description of the electronic structure of the system may have a sizable error (Figure 2 a). To our knowledge, the energies corrected for the CCSD(T) accuracy, $\Delta E_{CCSD(T)}$, are the most reliable theoretical data[28] presented for the deNO$_x$ processes. $\Delta E_{CCSD(T)}$ and ΔE_{B3LYP} are in good agreement for intermediates **7**–**8** whereas ΔE_{B3LYP} is below $\Delta E_{CCSD(T)}$ for species **1**–**6** up to 50 kJ mol^{-1}; the $\Delta E_{CCSD(T)}$ values represent the upper limit for the activation barriers.

Many authors have argued that deNO$_x$ reactions proceed on a pair of Cu^I sites: 1) in analogy with copper-containing proteins (a bis(μ-oxo)dicopper has been proposed to be an active catalytic site and identified by extended X-ray absorption fine structure (EXAFS) spectroscopy),[5] and 2) increased activity of the Cu/zeolite samples with larger Cu loading has been attributed to the presence of nearby Cu^I sites.[3,6,13] While these are strong arguments in favor of the involvement of a pair of Cu^I cations, there is solid experimental evidence against it: the turnover frequency (TOF, related to the number of Cu sites in the sample) is higher in zeolites with higher Si/Al ratios.[4,13,29] We cannot directly analyze the discrepancy described above since only the involvement of a single Cu^I site is considered in the present work. However, the results presented provide an alternative interpretation of the experimental data: increased activity of zeolites with higher Cu loading is not only due to the formation of Cu pairs but also due to the differences in Cu^I site activity (differences in the Cu^I coordination) in sites populated at an increasing ion-exchange level. Such a model is consistent with the experimental results of increased catalytic activity as both Cu loading and Si/Al ratio increases. There is however the requirements that copper is first exchanged into the sites where it can adopt an ideal coordination with the zeolite framework and the sites with less coordinated Cu^I are exchanged at higher Cu loadings, which have been evidenced for Cu/ZSM-5.[24]

In summary, we have investigated the reaction mechanism of NO decomposition catalyzed by Cu/zeolites, highlighting the role of the Cu^I coordination and localization in zeolites on the reaction profile. The improved coordination of the Cu^I

cation with the framework results in the formation of less stable reaction intermediates and in higher apparent energies of activation. We believe that this result is of general importance and improves our understanding of the structure–activity relationship.

Methods

A recent study of the structure and stability of various mono- and dinitrosyl complexes formed in Cu/FER has revealed that small- and medium-size cluster models may give incorrect relative energies for complexes formed on different Cu^I sites.[21] In addition, the PBE exchange–correlation functional was shown to overestimate the stability of mono- and dinitrosyl complexes on Cu^I.[21] To overcome these problems, the calculations presented here consist of the following steps:

1) The periodic DFT calculations employing the PBE exchange–correlation functional were performed on Cu/FER (unit cell (UC) composition CuAlSi$_{35}$O$_{72}$ and the dimensions from Ref. [30] were used; some calculations were performed with double UC) and on Cu/MFI (UC composition CuAlSi$_{95}$O$_{192}$ and the dimensions from Ref. [31] were used). A projector-augmented-wave method[32, 33] and plane wave basis set (with an energy cut-off of 400 eV) were used; the calculations were performed with the VASP program.[34] The optimization of the transition-state structures was performed with the dimer method using only the first derivatives as described previously[35, 36]. The energies are reported with respect to the energy of the reactants (bare Cu^I in the particular site in Cu/FER or Cu/MFI, denoted as ZCu, and two NO molecules in the gas phase). The relative energies calculated at the PBE level are referred to as ΔE_{PBE}. This level of theory was used for all of the geometry optimizations.

2) The relative energies calculated at the PBE level were corrected using a more reliable B3LYP functional; those energies corrected for B3LYP accuracy are denoted as ΔE_{B3LYP}. Corrections were performed as single-point energy calculations at the PBE and B3LYP levels on medium-size cluster models at the geometries obtained with the periodic PBE model (described above). Details about the cluster models and basis sets can be found in Ref. [21]; the calculations were performed with the Gaussian03 program.[37]

3) The coupled clusters method [CCSD(T)] was used for the coupled clusters corrected energies, $\Delta E_{CCSD(T)}$, obtained as single-point energy calculations at the B3LYP and CCSD(T) levels on the 1-T cluster model, (NO)$_2$CuAl(OH)$_4$, at the geometries obtained with the PBE functional (see Ref. [21] for details about the 1-T model and the basis sets used). The calculations were performed with the Molpro 06 program suite.[38]

4) For a comparison with the experimental data, the enthalpy changes were obtained from $\Delta E_{CCSD(T)}$ by adding the zero-point vibrational energy correction, $\Delta H = \Delta E_{CCSD(T)} + \Delta E_{ZPVE}$, where ΔE_{ZPVE} was evaluated within the harmonic approximation at the periodic PBE level employing a 15-dimensional model Hessian (considering all of the degrees of freedom for the Cu atom and for the N and O atoms involved in the reaction).

[1] M. Iwamoto, S. Yokoo, K. Sakai, S. Kagawa, *J. Chem. Soc. Faraday Trans.* **1981**, *77*, 1629.
[2] H. Yahiro, M. Iwamoto, *Appl. Catal. A* **2001**, *222*, 163.
[3] E. Giamello, D. Murphy, G. Magnacca, C. Morterra, Y. Shioya, T. Nomura, M. Anpo, *J. Catal.* **1992**, *136*, 510.
[4] G. Moretti, *Catal. Lett.* **1994**, *23*, 135.
[5] M. H. Groothaert, J. A. Vanbokhoven, A. A. Battiston, B. M. Weckhuysen, R. A. Schoonheydt, *J. Am. Chem. Soc.* **2003**, *125*, 7629.
[6] Y. Kuroda, M. Iwamoto, *Top. Catal.* **2004**, *28*, 111.
[7] I. I. Zakharov, Z. R. Ismagilov, S. P. Ruzankin, V. F. Anufrienko, S. A. Yashnik, O. I. Zakharova, *J. Phys. Chem. C* **2007**, *111*, 3080.
[8] Y. Kuroda, R. Kumashiro, T. Yoshimoto, M. Nagao, *Phys. Chem. Chem. Phys.* **1999**, *1*, 649.
[9] P. Spuhler, M. C. Holthausen, D. Nachtigallová, P. Nachtigall, J. Sauer, *Chem. Eur. J.* **2002**, *8*, 2099.
[10] G. Spoto, S. Bordiga, D. Scarano, A. Zecchina, *Catal. Lett.* **1992**, *13*, 39.
[11] S. Larsen, A. Aylor, A. Bell, J. Reimer, *J. Phys. Chem.* **1994**, *98*, 11533.
[12] B. Wichterlová, Z. Sobalik, J. Dedecek, *Catal. Today* **1997**, *38*, 199.
[13] P. Smeets, B. Sels, R. van Teeffelen, H. Leeman, E. Hensen, R. Schoonheydt, *J. Catal.* **2008**, *256*, 183.
[14] M. Iwamoto, H. Yahiro, N. Mizuno, W.-X. Zhang, Y. Mine, H. Furukawa, S. Kagawet, *J. Phys. Chem.* **1992**, *96*, 9360.
[15] P. Smeets, M. Groothaert, R. van Teeffelen, H. Leeman, E. Hensen, R. Schoonheydt, *J. Catal.* **2007**, *245*, 358.
[16] W. F. Schneider, K. C. Hass, R. Ramprasad, J. B. Adams, *J. Phys. Chem. B* **1998**, *102*, 3692.
[17] N. Tajima, M. Hashimoto, F. Toyama, A. M. El-Nahas, K. Hirao, *Phys. Chem. Chem. Phys.* **1999**, *1*, 3823.
[18] X. Solans-Monfort, M. Sodupe, V. Branchadell, *Chem. Phys. Lett.* **2003**, *368*, 242.
[19] D. Sengupta, J. B. Adams, W. F. Schneider, K. C. Hass, *Catal. Lett.* **2001**, *74*, 193.
[20] L. Rodriguez-Santiago, M. Sierka, V. Branchadell, M. Sodupe, J. Sauer, *J. Am. Chem. Soc.* **1998**, *120*, 1545.
[21] A. Pulido, P. Nachtigall, *Phys. Chem. Chem. Phys.* **2009**, *11*, 1447.
[22] D. Nachtigallová, P. Nachtigall, M. Sierka, J. Sauer, *Phys. Chem. Chem. Phys.* **1999**, *1*, 2019.
[23] M. Davidová, D. Nachtigallová, P. Nachtigall, J. Sauer, *J. Phys. Chem. B* **2004**, *108*, 13674.
[24] R. Bulánek, P. Cicmanec, P. Knotek, D. Nachtigallová, P. Nachtigall, *Phys. Chem. Chem. Phys.* **2004**, *6*, 2003.
[25] Y. J. Li, W. K. Hall, *J. Catal.* **1991**, *129*, 202.
[26] F. Garin, *Appl. Catal. A* **2001**, *222*, 183.
[27] G. Herzberg, in *Molecular Spectra and Molecular Structure, Vol. 3, Electronic Spectra and Electronic Structures of Polyatomic Molecules*, Van Nostrand, New York, **1966**.
[28] K. Koszinowski, D. Schroder, H. Schwarz, M. C. Holthausen, J. Sauer, H. Koizumi, P. B. Armentrout, *Inorg. Chem.* **2002**, *41*, 5882.
[29] L. Lisi, R. Pirone, G. Ruoppolo, G. Russo, *Kinet. Catal.* **2008**, *49*, 421.
[30] O. Bludský, M. Silhan, P. Nachtigall, T. Bucko, L. Benco, J. Hafner, *J. Phys. Chem. B* **2005**, *109*, 9631.
[31] C. O. Arean, M. R. Delgado, K. Frolich, R. Bulanek, A. Pulido, G. F. Bibiloni, P. Nachtigall, *J. Phys. Chem. C* **2008**, *112*, 4658.
[32] P. E. Blöchl, *Phys. Rev. B* **1994**, *50*, 17953.

[33] G. Kresse, D. Joubert, *Phys. Rev. B* **1999**, *59*, 1758.

[34] G. Kresse, J. Furthmuller, *Phys. Rev. B* **1996**, *54*, 11169.

[35] G. Henkelman, H. Jonsson, *J. Chem. Phys.* **1999**, *111*, 7010.

[36] http://theory.cm.utexas.edu/vtsttools/.

[37] M. J. Frisch, et al., Gaussian Inc., Pittsburgh PA, **2003**.

[38] H.-J. Werner, et al., MOLPRO, version 2006.1, **2006**.